Separation of Single-Walled Carbon Nanotubes by 1-Dodecanol-Mediated Size-Exclusion Chromatography

Benjamin S. Flavel,[†,*] Manfred M. Kappes,[†,‡] Ralph Krupke,[†,§] and Frank Hennrich[†,*]

[†]Institute of Nanotechnology, Karlsruhe Institute of Technology, 76021 Karlsruhe, Germany, [‡]Institute of Physical Chemistry, Karlsruhe Institute of Technology, 76128 Karlsruhe, Germany, and [§]Institute of Materials Science, Technische Universität Darmstadt, 64287 Darmstadt, Germany

ABSTRACT A simple, single-column, high-throughput fractionation procedure based on size-exclusion chromatography of aqueous sodium dodecyl sulfate suspensions of single-walled carbon nanotubes (SWCNTs) is presented. This procedure is found to yield monochiral or near monochiral SWCNT fractions of semiconducting SWCNTs. Unsorted and resulting monochiral suspensions are characterized using optical absorption and photoluminescence spectroscopy.

KEYWORDS: carbon nanotubes · gel filtration · size-exclusion chromatography · separation · sorting · purification

Development and application of separation techniques for the fractionation of single-walled carbon nanotube (SWCNTs) is an active ongoing research field. Current research efforts are driven by the absence of a single synthesis method capable of affording carbon nanotube samples of preselected electronic type (metallic (m) or semiconducting (s)), diameter (d_t), chiral angle, or (n,m) index. Typically, SWCNTs are synthesized by techniques such as arc discharge, laser ablation, or the HiPco process, wherein a complex mixture of many different SWCNTs, described by a distribution of chiral indices (n,m), is obtained. Therefore, the separation of SWCNTs by fractionation of (n,m) species is an important, application-oriented goal. Previously, separation has been achieved by various groups utilizing such techniques as the wrapping of SWCNTs with short sequences of single-stranded DNA (ssDNA) and subsequent ion exchange chromatography (IEX),[1] the suspension of SWCNTs with surfactants followed by density gradient centrifugation[2−4] (DGC) or gel filtration.[5−7]

However, it is the Sephacryl gel filtration/size-exclusion chromatography (SEC) method developed by Moshammer *et al.*[4] that is the most straightforward and allows for high-throughput separation of m- from s-SWCNTs. This method relies upon the use of SWCNTs suspended in aqueous sodium dodecyl sulfate (SDS) and has also been shown to enrich zigzag and (n,0) SWCNTs.[5] Recently Liu *et al.*[3] further improved the sorting of SWCNTs with SEC to include the addition of starting SDS-SWCNT suspensions to a series of gel columns and were capable of isolating 13 different (n,m) species.

Despite recent success, the mechanism of SWCNT separation by (n,m) species with gel filtration/SEC remains unclear. SEC is known to separate nanoscale objects passing through a column according to *differences in their size* and has been extensively used to *size-separate* SWCNTs. It was therefore proposed by Moshammer *et al.*[4] that the observed m/s-SWCNT separation is reliant upon appropriate initial dispersion of the raw SWCNT material by sonication, with the dispersion of SWCNTs in SDS shown to be selective to electronic structure. In fact, aqueous SDS starting suspensions obtained after sonication of SWCNT raw material were found to primarily contain s-SWCNTs in the form of bundles with m-SWCNTs predominantly suspended as individual tubes.[4] Upon introduction of the SWCNT-SDS suspension

* Address correspondence to benjamin.flavel@partner.kit.edu, frank.hennrich@kit.edu.

Received for review January 30, 2013 and accepted March 29, 2013.

Published online March 29, 2013
10.1021/nn4004956

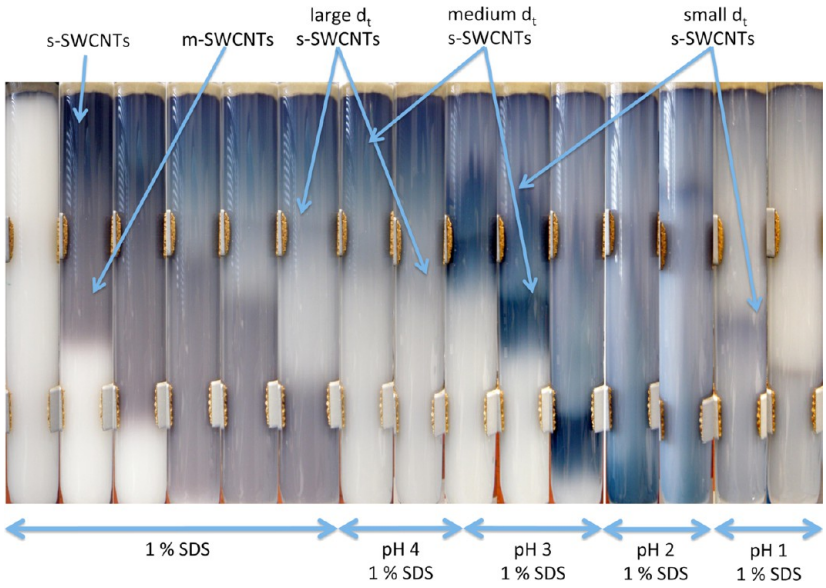

Figure 1. Time lapse photography of HiPCo SWCNTs suspended in 1 wt % SDS in H_2O on a Sephacryl S-200 size-exclusion gel, followed by subsequent reductions of pH.

to a size-exclusion gel medium, the bundles (s-SWCNTs) could therefore be easily separated from the individual (m-SWCNTs) tubes on the basis of their hydrodynamic size difference. By choosing an appropriate column medium, particle size, gel porosity, and eluent composition, it was therefore possible to run the SEC column as a "filter", with the longer, rigidly bundled s-SWCNTs becoming trapped on the gel and the smaller individualized m-SWCNTs being eluted in a 1 wt % SDS solution. Trapped s-SWCNTs were then removed from the gel by eluent exchange to 1 wt % SChol (sodium cholate). It is then the increased dispersibility of SWCNTs in SChol that allows for trapped s-SWCNTs to be further individualized and elute.

In the method of Liu *et al.*,[3] rather than changing the eluent medium, the wt % concentration of SDS was altered from 2 to 5%, allowing for the separation of 13 different (*n*,*m*) species. The authors explain their ability to then wash individual (*n*,*m*) s-SWCNT species from the gel by (*n*,*m*)-specific variations in the SDS coating of SWCNTs. These variations are proposed to be a result of differences in the surface π-electron states pertaining to individual (*n*,*m*) species (due to differing bond curvature), which alters the interaction between s-SWCNTs and SDS. Thereby, this results in a strongly curvature-dependent (*n*, *m*) separation method.

In this contribution, we demonstrate that Sephacryl S-200, an allyl dextran-based size-exclusion gel, can be used as a stationary phase such that monochiral or near monochiral SWCNTs can be simply produced on one column by altering the pH of the eluent. This, in turn, allows simple fractionation of (*n*,*m*)-pure or almost (*n*,*m*)-pure SWCNT suspensions from the total s-SWCNT population.

RESULTS AND DISCUSSION

As outlined in the Methods section, the high-throughput separation of (*n*,*m*)-pure s-SWCNTs with a single-column SEC approach involved the following steps: Initially, a 1 wt % SDS in H_2O suspension of raw HiPco-SWCNT material was added to a Sephacryl S-200 gel bed under 1 wt % SDS in H_2O. Upon addition of further 1 wt % SDS in H_2O, the m-SWCNTs were eluted from the column. This process can be seen in the time lapse photography in Figure 1, wherein the s-SWCNTs (blue-green color) can be seen clearly trapped on the top of the column in the gel while the m-SWCNTs (red-brown color) move through the gel.

This resulted in the establishment of essentially stationary colored bands on the Sephacryl gel, where the top to middle region of the gel is characterized by a color gradient of purple-blue to green-yellow. After complete separation of m- from s-SWCNTs, the pH of the 1 wt % SDS eluent solution was reduced from pH 7 to 1 in decrements of 1 pH level. Upon reaching pH 4, the trapped s-SWCNTs can be seen to separate into different colored moving eluent bands. The resolution of these bands was then improved upon further reduction of pH, with yellow, green, blue, and purple bands afforded for pH 4, 3, 2, and 1, respectively. Within the raw HiPco starting material, these bands corresponded to comparably large (yellow) to medium (green and blue) to small (purple) SWCNT diameters (d_t). This effect can be more precisely seen by absorption spectroscopy in Figure 2a, where the unsorted HiPco material is compared to fractions obtained at each pH level for the first optical transition (S_{11}) between 850 and 1350 nm. Complete absorbance spectra displaying both the first (S_{11}) and second (S_{22}) optical transitions between 500 and 1350 nm

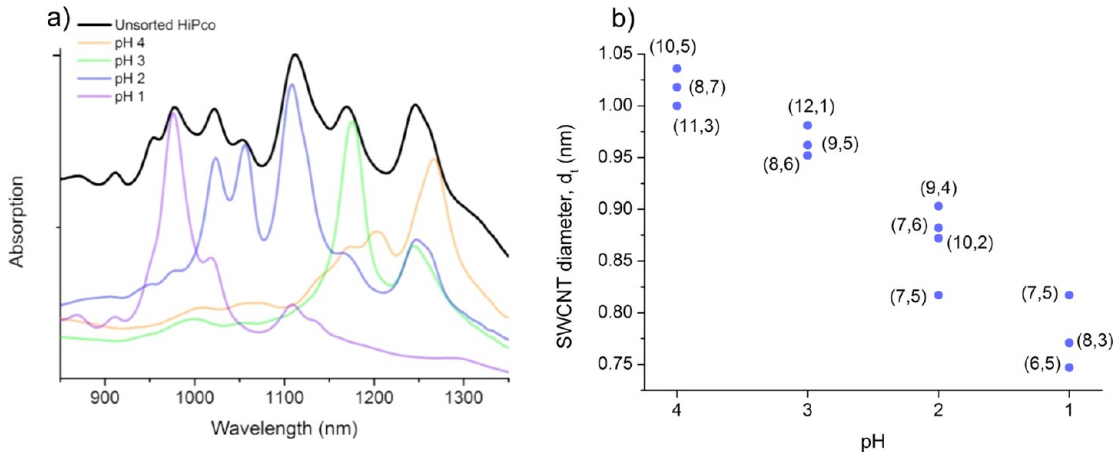

Figure 2. (a) Absorption spectra of unsorted HiPco material and fractions obtained at pH 4−1 in 1 wt % SDS and (b) SWCNT diameter dependence upon pH.

can also be found in Figure 1 of the Supporting Information. Due to the well-known doping effect[8] and subsequent quenching of the S_{11} optical transition, all fractions were neutralized to pH 7 in a 1 wt % SDS solution by dialysis prior to measurement.

Each fraction was found by photoluminescence spectroscopy to contain predominantly three individual (*n*,*m*) species; however, it is important to note that the displayed fractions only represent a "snapshot" of many fractions obtained at each pH level. Corresponding photoluminescence contour maps for each fraction can also be found in Figure 2 of the Supporting Information. The SWCNT diameter (d_t) of these species was then obtained by reference to the photoluminescence data of Weisman *et al.*[9] and is shown in Figure 2b, where it can be seen that d_t decreases with eluent pH. Upon summation of each (*n*,*m*) species diameter in a collected fraction, this trend is clearly seen with average d_t found to be 1.018, 0.957, 0.868, and 0.778 nm for pH 4, 3, 2, and 1, respectively.

The ability of this method to generate monochiral or near monochiral SWCNT suspensions was then realized by slowly changing the pH from 4 to pH 1 in 12, 25% reductive steps. In order to easily visualize the obtained fractions, photoluminescence spectroscopy was then used and is shown in Figure 3. Additionally, absorption spectra of each fraction are shown in Figure 4a. Furthermore, to allow comparison, a photoluminescence contour map of the unsorted HiPco SWCNT material is shown in Figure 3 of the Supporting Information, wherein 17 different (*n*,*m*) species are clearly visible. As found for coarse reductions in pH, the d_t of the collected SWCNT fractions were once again observed to decrease with pH, as shown in Figure 4b. However, in this instance, due to slight variations in the pH of the 1 wt % SDS eluent added to the top of the column and the establishment of a pH gradient across the column, it is more difficult to determine the true pH of each fraction. Therefore "elution order" is used, where fractions eluted later are obtained at relatively lower pH values compared to earlier fractions. To aid the eye, only the major (*n*,*m*) contribution is plotted in Figure 4b. Nanotube purity was then determined by the relative peak intensities of the contour map (uncorrected for the chiral-dependent quantum yield). Furthermore, the fitted peak area of absorption measurements was also used to calculate (*n*,*m*) purity, where the major (*n*,*m*) contribution was taken as a ratio of all other peaks.

As shown in Table 1, sorting of raw HiPco SWCNT material with pH variation resulted in the obtainment of 12 of the 17 (*n*,*m*) species with purities between 23 and 86%. The reduced purity level for absorption measurements is a result of the difficulty in accurately performing the peak fitting procedure in a region with many overlapping first interband transitions. The actual (*n*,*m*) purity is expected to lie between the value obtained from photoluminescence and that from absorption measurements. For an effective sorting method, it is also important to assess the yield of the various (*n*,*m*) species. While we did not measure this directly, it is noted that the starting solution has a dispersed SWCNT mass of approximately 1 mg and the final (*n*,*m*) fractions were in the microgram range. It should also be noted that between 450 and 550 nm, nanotube-related transitions are clearly seen in the absorption spectra. This absorption regime is typically associated with m-SWCNTs; however, due to an overlap of the third interband transition of HiPco s-SWCNTs and the first interband transition of HiPco m-SWCNTs, it is difficult to estimate the concentration of m-SWCNTs. However, preliminary electrical transport measurements indicate a metallic-/semiconducting-SWCNT ratio equivalent to standard Sephacryl S-200 separations. Despite being unable to achieve separations of the same purity as Liu *et al.*,[3] who were able to obtain 13 different (*n*,*m*) species with purities between 39 and 94%, the sorting of s-SWCNTs by pH variation presented in this work has the advantage of requiring a single SEC column, which significantly decreases the

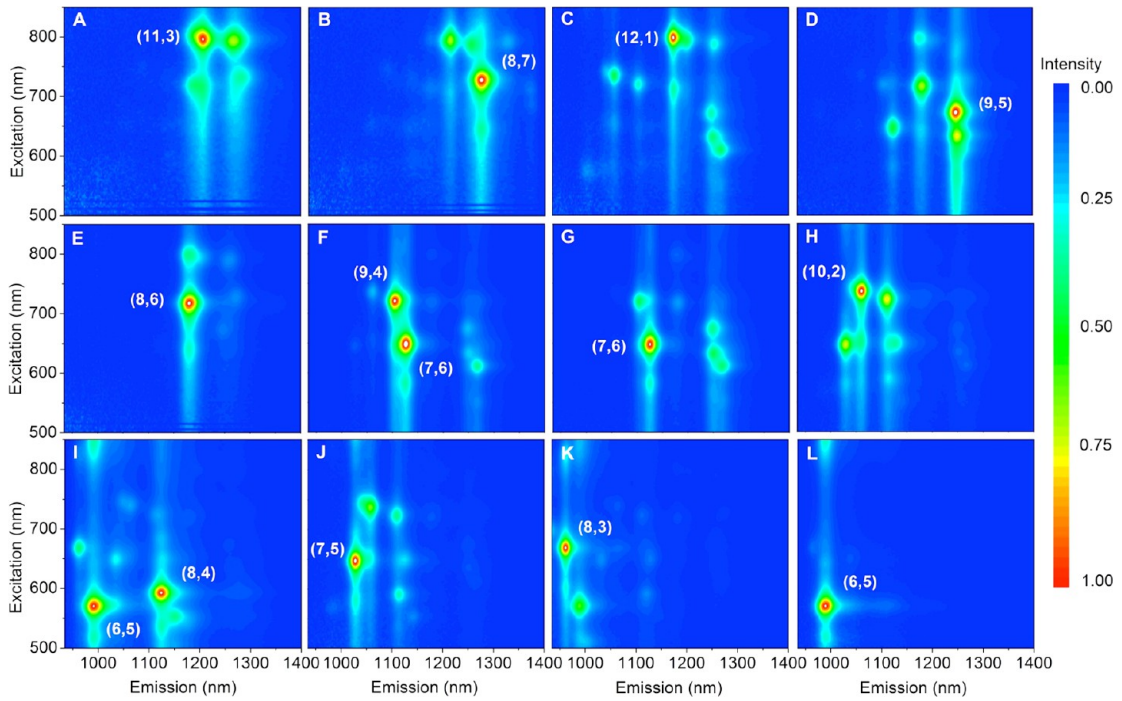

Figure 3. Photoluminescence contour maps of fractions (elution order A−L) obtained upon reducing the 1 wt % SDS eluent from pH 4 to pH 1 in 12 reductive steps.

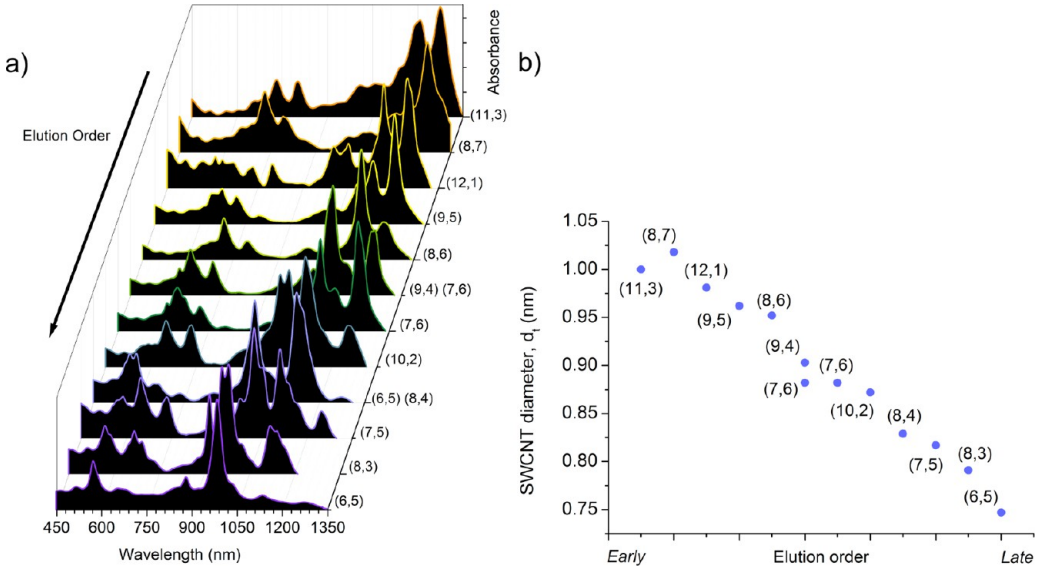

Figure 4. (a) Absorption spectra corresponding to fractions displayed in Figure 3 and (b) SWCNT diameter dependence upon elution order.

TABLE 1. Maximum Obtained Purity of Enriched (*n*,*m*) Species by Reducing the pH of the Eluent

(*n*,*m*) species	(6,5)	(7,5)	(7,6)	(8,3)	(8,4)	(8,6)	(8,7)	(9,4)	(9,5)	(10,2)	(11,3)	(12,1)
photoluminesence, purity (%)	86	40	38	46	30	57	44	32	35	30	41	28
absorption, purity (%)	72	27	27	19	25	64	37	19	32	17	19	23

complexity of the separation process. Additionally, the elution order of Liu *et al.*[3] (small to large diameter) appears to be opposite to the order observed in this work (large to small). However, it is important to remember that Liu *et al.* determined their elution order by considering the nanotube of strongest interaction with the gel (small diameter), which due to their multiple short-column approach results in it being the first

collected species. In this work, we see the same trend, with strongly (small diameter) and weakly (large diameter) absorbed species located at the uppermost and midpoint of a single long column, respectively (Figure 1). Upon reduction of the pH, the established on-column nanotube ordering is maintained, and large to small diameter nanotube fractions are collected. Therefore, it is purely the experimental approach and definition of "first eluent" that results in a perceived difference.

Despite the mechanism responsible for the separation of (*n*,*m*) s-SWCNT species ultimately remaining unclear, we next provide an attempt to elucidate the most likely cause upon consideration of the SDS surfactant shell structure on nanotubes and similar carbon surfaces and the subsequent effect of pH. The morphology of SDS aggregates on graphite is well-known, with theoretical calculations and contact AFM measurements revealing the sp^2 carbon lattice to serve as a template for the organization of surfactant chains, which is responsible for defining the surfactant micelle morphology.[10−15] SDS micelles are found as ordered linear, parallel aggregates, which are oriented perpendicular to an underlying symmetry axis and spaced slightly more than twice the surfactant molecular length apart. These initially adsorbed molecules then act as nucleation sites for the growth of the hemispherical micelles, wherein adjacent molecules are oriented tail to tail, forming parallel semicylindrical rows, with tail groups oriented parallel to the symmetry axis.

On the other hand, the SDS micelle morphology for CNTs remains under debate with various theoretical groups proposing disordered[10] and ordered[16,17] structure. Experimentally, Yurekli *et al.*[18] also measured small-angle neutron scattering (SANS) of aqueous SDS-SWCNT suspensions and found SDS to form disordered aggregates. Alternatively, Richard *et al.*[19] with the use of cryo-TEM measurements found SDS to form hemispherical micelles on the sidewall of multiwalled nanotubes. However, common to all work is a strong dependence of the micelle structure on surfactant concentration and nanotube diameter. For partial SDS surfactant coverage (1.0 molecules/nm), Xu *et al.*[14] theoretically found SDS to be disordered for small (6,6) and large (18,18) or (30,30) d_t SWCNTs. Upon reaching full coverage (2.8 molecules/nm), they then found SDS to form stable hemispherical micelles for large (18,18) or (30,30) d_t SWCNTs, a result that is in agreement with the experimental work on graphite and multiwalled carbon nanotubes. For small (6,6) d_t SWCNTs and in agreement with the work of Wallace *et al.*,[20] SDS was found to form a cylinder-like monolayer micelle, in which the carbon nanotube forms the core with the surfactant extended radially from the center. It was therefore concluded that SDS hemispherical micelle ordering occurs on carbon nanotubes only in the case of high surfactant concentration and large diameter. Furthermore, Niyogi *et al.* have demonstrated m-SWCNTs to have a higher packing density (concentration) of SDS compared to s-SWCNTs,[21] which may therefore imply a higher degree of SDS ordering.

However, the morphology of the SDS micelle structure has also been shown to be susceptible to changes in the surrounding environment, with the addition of organic molecules or electrolyte tuning capable of surfactant shell modification.[19,22,23] Toward this end, upon reduction of pH, the presence of H^+ ions has been shown to lead to the hydrolysis of SDS between pH 2 and pH 3, which results in the formation of 1-dodecanol[24] as given by eq 1.

$$C_{12}H_{25}OSO_3^- + H_2O \rightarrow C_{12}H_{25}OH + HSO_4^- \quad (1)$$

This hydrolysis mechanism is the cause of the well-known long-term instability of SDS and can also be initiated by heating.[22] Parachuri *et al.* have used AFM to show the addition of 5 mM 1-dodecanol to 100 mM SDS to cause significant structural changes in the continuous parallel semicylindrical surface micelle structure on graphite surfaces.[8,9] It is shown that the parallel semicylindrical structure is replaced by a herringbone pattern upon integration of 1-dodecanol into the micelle structure. If it is assumed (in agreement with Xu *et al.*[14]) that SDS forms semicylindrical micelles on the surface of carbon nanotubes, then a similar structural rearrangement can be expected for the SWCNT micelle upon addition of 1-dodecanol.

Such structural changes will then have a strong influence on the SWCNT's interaction with its surrounding environment. The total interaction of SWCNTs on the Sephacryl gel is strongly dependent upon van der Waals forces between the SWCNTs and the gel as well as steric and electrostatic interactions. Any differences in surfactant structure will therefore affect this interaction. For example, it is well-known that electrostatic interactions can occur between charged solutes and charged SEC packing materials. Sun *et al.*[25] conducted zeta-potential measurements of SDS-SWCNT suspensions and found the presence of SDS to lead to a net negative charge, which upon addition of neutral 1-dodecanol is likely reduced, which in turn would reduce the SWCNT interaction with the gel and cause nanotube elution. Alternatively, SEC is by definition a chromatographic process, which is capable of separating particles based on their hydrodynamic volume. The introduction of 1-dodecanol may either alter the hydrodynamic volume of individual tubes or have a debundling effect, likewise altering the hydrodynamic volume, as discussed in our previous work[4,5] where a surfactant change to sodium cholate is required for nanotube elution.

We therefore propose that during SWCNT starting suspension preparation with extended ultrasonication, a low concentration of 1-dodecanol is produced by microcavitation (heat), which is then integrated into

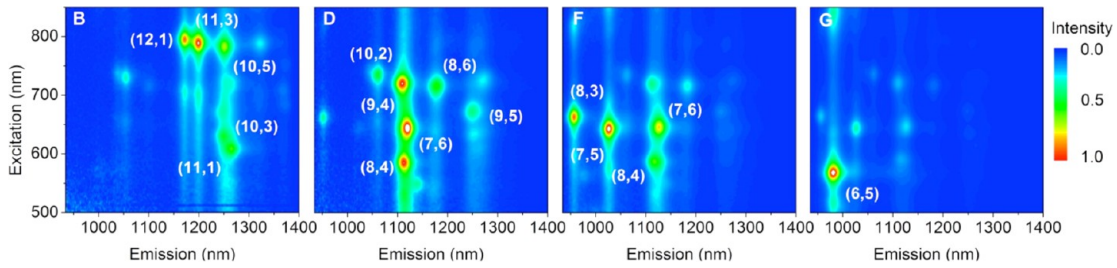

Figure 5. Photoluminescence contour maps of fractions (elution order A–G) upon addition of 5 μM 1-dodecanol to the starting HiPco raw material.

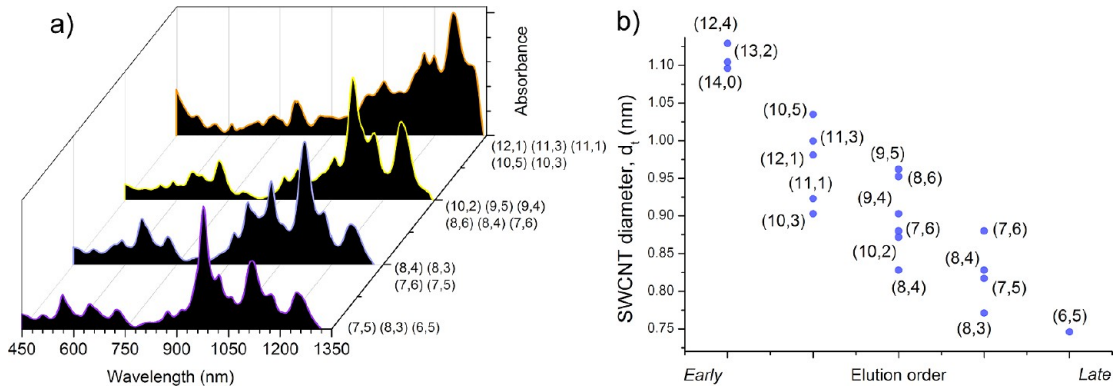

Figure 6. SWCNT diameter dependence upon elution order upon addition of 5 μM 1-dodecanol to the starting HiPco raw material.

the SDS-SWCNT hemimicellar structure. The resultant structural change alters the interaction of the SWCNTs, allowing them to move through the Sephacryl gel. As the sonicated SWCNTs are added to a freshly prepared 1 wt % SDS-filled gel column and further washed through with fresh 1 wt % SDS, the initial concentration of 1-dodecanol is quickly depleted and the nanotubes become trapped on the gel. It is also proposed, and in agreement with literature,[18] that metallic nanotubes have a higher SDS coverage compared to semiconducting nanotubes and hence have a higher degree of surfactant ordering and are therefore capable of integrating more 1-dodecanol and thereby move further and faster in the gel. This results in the observed metallic/semiconducting separation. The m-SWCNTs are either debundled[4,5] or have a significantly reduced electrostatic interaction with the gel as a result of the 1-dodecanol. A similar argument is also made for large and small diameter SWCNTs, where the increased integration of 1-dodecanol allows large diameter s-SWCNTs to move further in the column prior to stopping. Upon depletion of 1-dodecanol the s-SWCNTs either bundle together[4,5] or have an increased electrostatic interaction with the gel. Upon reducing the pH of the 1 wt % SDS solution, 1-dodecanol is then reintroduced by hydrolysis and allows the trapped s-SWCNTs to elute.

This model is supported by the following experiments. First, we repeated the separation of raw HiPco SWCNT material by adding increasing concentrations of 1-dodecanol to the pH-neutral, 1 wt % SDS eluent. Once again, the s-SWCNTs were trapped on the top half of the Sephacryl gel. Upon increasing the 1-dodecanol concentration in 1 μM steps to a final concentration of 5 μM, these SWCNTs could then be eluted in order of comparatively large to small d_t, as expected (data not shown). Second and alternatively, 5 μM 1-dodecanol was added to the raw starting material, which was then subsequently added to a Sephacryl gel column under 1 wt % SDS and further washed with fresh 1 wt % SDS. In this instance, the s-SWCNTs did not become trapped on the SEC gel (for a short column). However, the m-SWCNTs once again moved faster through the gel compared to large d_t s-SWCNTs, which in turn moved faster than small d_t s-SWCNTs. In this way, a metallic/semiconducting separation plus a s-SWCNT diameter separation was achieved in *one* step without changing surfactant, pH, or column. In addition to being extremely simple, this method also has the added benefit of not clogging the gel with trapped, unmoveable, s-SWCNTs, hence dramatically increasing column lifetime. Corresponding photoluminescence contour maps are shown in Figure 5 and Supporting Information Figure 4, with elution order A–G, and absorption spectra in Figure 6a. The diameter-dependent elution order is then more precisely seen in Figure 6b. Alternatively, the raw material was added to a column containing 5 μM 1-dodecanol in 1 wt % SDS; however, the excess of alcohol leads to all SWCNT species moving together without separation and highlights the importance of a 1-dodecanol gradient.

TABLE 2. Maximum Obtained Purity of Enriched (*n*,*m*) Species from the Addition of 5 μM 1-Dodecanol to the Raw HiPco SWCNT Material

(*n*,*m*) species	(6,5)	(7,5)	(7,6)	(8,3)	(8,4)	(9,4)	(10,2)	(10,5)	(11,3)	(12,1)	(12,4)	(13,2)
photoluminesence, purity (%)	50	26	22	22	20	18	28	16	25	21	16	32

Once again, aggregation of photoluminescence peak intensities allowed for the determination purity, as shown in Table 2. Furthermore, the additional photoluminescence contour maps found in Figure 4 of the Supporting Information allowed the concentration of the (13,2), (12,4), (10,2), and (9,4) s-SWCNTs to be determined. Additional to the (*n*,*m*) species obtained by pH sorting, the (10,5), (12,4), and (13,2) were also purified, resulting in a total of 15 out of the total 17 available (*n*,*m*) species being sorted in this work. Unfortunately, in comparison to fractions obtained from pH sorting, the purity of (*n*,*m*) species obtained from 1-dodecanol addition was found to be lower (between 16 and 50%). This is presumably due to the addition of 1-dodecanol resulting in a dynamic process without the static equilibration of SWCNT diameters across the gel prior to the beginning of the experiment. Furthermore, it should be noted that SWCNT separations from 1-dodecanol only serve as a proof of principle and provide insights into the mechanism responsible for SWCNT separation by pH variation. It is expected that after extensive optimization of the 1-dodecanol concentration s-SWCNT suspensions similar to those obtainable from pH variation will be achievable.

CONCLUSION

In conclusion, we have shown the (*n*,*m*) separation of 15 different nanotube species with a purity of 16−93%. Furthermore, sorting was achieved conveniently and simply in a single Sephacryl column without the need for a surfactant/eluent change. Upon tailoring the concentration of 1-dodecanol through reduction of pH or the direct addition of alcohol to the raw starting material, the originally strong interaction of s-SWCNT could be reduced and allowed for diameter-dependent fractionation.

METHODS

A brief description of the experimental methods is as follows. HiPco SWCNT raw material (NanoIntegris) was used in this work. In order to prepare starting suspensions, typically 10 mg of raw SWCNT material was suspended in 15 mL of H_2O with 1 wt % of SDS using a tip sonicator (Bandelin, 200 W maximum power, 20 kHz, in pulsed mode with 100 ms pulses) applied for 2 h at ∼20% power. During sonication, the suspension was placed in a 500 mL water bath without additional cooling. The resulting dispersion was then centrifuged at ∼100 000*g* for 1.5 h and carefully decanted from the pellet which was formed during centrifugation. The centrifuged SWCNT suspension was used as the "starting suspension" for gel filtration fractionation as described below.

A separate "reference suspension" of the raw HiPco SWCNTs was made by suspending 10 mg of raw SWCNTs in 15 mL of H_2O with 1 wt % of sodium cholate. After tip sonication, the suspensions were centrifuged at 100 000*g* for 1 h, and the suspension was carefully decanted of the supernatant.

Gel filtration was performed as described previously[4] using a Sephacryl S-200 (manufacturer stated stability to pH of between 2 and 13) gel filtration medium (Amersham Biosciences) in a glass column of 20 cm length and 2 cm inner diameter. After filling the glass column with the filtration medium, the gel was slightly compressed to yield a final height of ∼14 cm. For the separation, ∼10 mL of SWCNT starting suspension was applied to the top of the column, and subsequently, a solution of 1 wt % SDS in H_2O as eluent was pushed through the column by applying sufficient pressure with compressed air to ensure a flow of ∼1 mL/min. After ∼10 mL of 1 wt % eluent had been added to the column, most of the m-SWCNTs had moved through the column, whereas the s-SWCNTs remained trapped in the upper part of the gel. After applying a total of ∼120 mL of SDS solution in this fashion, the metallic tubes were completely removed from the gel. The pH of the 1 wt % SDS in H_2O eluent was then changed from 4 to 1 upon addition of the appropriate concentration of HCl. The pH was reduced in 12 steps, whereby at each step 80 mL of eluent was applied to the gel. The s-SWCNTs subsequently eluted from the column were collected separately in 2 mL fractions.

For spectroscopic characterization, gel filtration fractions were subsequently dialyzed for 24 h to readjust the pH to 7 in 1 mL Float-A-Lyzer G2 dialysis devices (Spectra-Por) by using 500 mL of a 1 wt % SDS solution in water. UV−vis−NIR absorption spectra of the dialyzed fractions were recorded on a Varian Cary 500 spectrophotometer. Photoluminescence maps were measured in the emission range of ∼900−1700 nm and excitation range of 500−950 nm (scanned in 3 nm steps) using a modified FTIR spectrometer (Bruker IFS66) equipped with a liquid-nitrogen-cooled Ge-photodiode and a monochromatized excitation light source as described elsewhere.[26]

Conflict of Interest: The authors declare no competing financial interest.

Acknowledgment. This research was supported by the Bundesministerium für Bildung und Forschung (BMBF) as administered by POF-NanoMicro. B.S.F. gratefully acknowledges the support of the Alexander von Humboldt Foundation.

Supporting Information Available: Absorption spectra of fractions obtained at pH 4−1 displaying the second interband transition (S_{22}), additional photoluminescence spectra of fractions obtained from variations in pH and the addition of 1-dodecanol, photoluminescence and absorption measurements of the raw/unsorted HiPco SWCNT material. This material is available free of charge *via* the Internet at http://pubs.acs.org.

REFERENCES AND NOTES

1. Tu, X.; Manohar, S.; Jagota, A.; Zheng, M. DNA Sequence Motifs for Structure-Specific Recognition and Separation of Carbon Nanotubes. *Nature* **2009**, *460*, 250–253.
2. Ghosh, S.; Bachilo, S. M.; Weisman, R. B. Advanced Sorting of Single-Walled Carbon Nanotubes by Nonlinear Density-Gradient Ultracentrifugation. *Nat. Nanotechnol.* **2010**, *5*, 443–450.
3. Arnold, M. S.; Green, A. A.; Hulvat, J. F.; Stupp, S. I.; Hersam, M. C. Sorting Carbon Nanotubes by Electronic Structure *via* Density Differentiation. *Nat. Nanotechnol.* **2006**, *1*, 60–65.

4. Arnold, M. S.; Stupp, S. I.; Hersam, M. C. Enrichment of Single-Walled Carbon Nanotubes by Diameter in Density Gradients. *Nano Lett.* **2005**, *5*, 713–718.
5. Liu, H.; Daisuke Nishide, D.; Tanaka, T.; Kataura, H. Large-Scale Single-Chirality Separation of Single-Wall Carbon Nanotubes by Simple Gel Chromatography. *Nat. Commun.* **2011**, *2*, 1–8.
6. Moshammer, K.; Hennrich, F.; Kappes, M. M. Selective Suspension in Aqueous Sodium Dodecyl Sulfate According to Electronic Structure Type Allows Simple Separation of Metallic from Semiconducting Single-Walled Carbon Nanotubes. *Nano Res.* **2009**, *2*, 599–606.
7. Blum, C.; Stürzl, N.; Hennrich, F.; Lebedkin, S.; Heeg, S.; Dumlich, H.; Reich, S.; Kappes, M. M. Selective Bundling of Zigzag Single-Walled Carbon Nanotubes. *ACS Nano* **2011**, *5*, 2847–2854.
8. Strano, M.; Huffman, C. B.; Moore, V. C.; O'Connell, M. J.; Haroz, E. H.; Hubbard, J.; Miller, M.; Rialon, K.; Kittrell, C.; Ramesh, S.; Hauge, R. H.; Smalley, R. E. Reversible, Band-Gap-Selective Protonation of Single-Walled Carbon Nanotubes in Solution. *J. Phys. Chem. B* **2003**, *107*, 6979–6985.
9. Weisman, R. B.; Bachilo, S. M. Dependence of Optical Transition Energies on Structure for Single-Walled Carbon Nanotubes in Aqueous Suspension: An Empirical Kataura Plot. *Nano Lett.* **2003**, *3*, 1235–1238.
10. Paruchuri, V. K.; Nalaskowski, J.; Shah, D. O.; Miller, J. D. The Effect of Co-surfactants on Sodium Dodecyl Sulfate Micellar Structures at a Graphite Surface. *Colloids Surf., A* **2006**, *272*, 157–163.
11. Paruchuri, V. K.; Nguyen, A. V.; Miller, J. D. Zeta-Potentials of Self-Assembled Surface Micelles of Ionic Surfactants Adsorbed at Hydrophobic Graphite Surfaces. *Colloids Surf., A* **2004**, *250*, 519–526.
12. Tummala, N. R.; Striolo, A. Role of Counterion Condensation in the Self-Assembly of SDS Surfactants at the Water Graphite Interface. *J. Phys. Chem. B* **2008**, *112*, 1987–2000.
13. Sammalkorpi, M.; Panagiotopoulos, A. Z.; Haataja, M. Structure and Dynamics of Surfactant and Hydrocarbon Aggregates on Graphite: A Molecular Dynamics Simulation Study. *J. Phys. Chem. B* **2008**, *112*, 2915–2921.
14. Dominguez, H. Self-Aggregation of the SDS Surfactant at a Solid−Liquid Interface. *J. Phys. Chem. B* **2007**, *111*, 4054–4059.
15. Wanless, E. J.; Ducker, W. A. Organization of Sodium Dodecyl Sulfate at the Graphite−Solution Interface. *J. Phys. Chem.* **1996**, *100*, 3207–3214.
16. Xu, Z.; Yang, X.; Yang, Z. A Molecular Simulation Probing of Structure and Interaction for Supramolecular Sodium Dodecyl Sulfate/Single-Wall Carbon Nanotube Assemblies. *Nano Lett.* **2010**, *10*, 985–991.
17. Islam, M. F.; Rojas, E.; Bergey, D. M.; Johnson, A. T.; Yodh, A. G. High Weight Fraction Surfactant Solubilization of Single-Wall Carbon Nanotubes in Water. *Nano Lett.* **2003**, *3*, 269–273.
18. Yurekli, K.; Mitchell, C. A.; Krishnamoorti, R. Small-Angle Neutron Scattering from Surfactant-Assisted Aqueous Dispersions of Carbon Nanotubes. *J. Am. Chem. Soc.* **2004**, *126*, 9902–9903.
19. Richard, C.; Balavoine, F.; Schultz, P.; Ebbesen, T. W.; Mioskowski, C. Supramolecular Self-Assembly of Lipid Derivatives on Carbon Nanotubes. *Science* **2003**, *300*, 775–778.
20. Wallace, E. J.; Sansom, M. S. P. Carbon Nanotube/Detergent Interactions *via* Coarse-Grained Molecular Dynamics. *Nano Lett.* **2007**, *7*, 1923–1928.
21. Niyogi, S.; Densmore, C. G.; Doorn, S. K. Electrolyte Tuning of Surfactant Interfacial Behavior for Enhanced Density-Based Separations of Single-Walled Carbon Nanotubes. *J. Am. Chem. Soc.* **2008**, *131*, 1144–1153.
22. Silvera-Batista, C. A.; Scott, D. C.; McLeod, S. M.; Ziegler, K. J. A Mechanistic Study of the Selective Retention of SDS-Suspended Single-Wall Carbon Nanotubes on Agarose Gels. *J. Phys. Chem. C* **2011**, *115*, 9361–9369.
23. Wang, R. K.; Chen, W.-C.; Campos, D. K.; Ziegler, K. J. Swelling the Micelle Core Surrounding Single-Walled Carbon Nanotubes with Water Immiscible Organic Solvents. *J. Am. Chem. Soc.* **2008**, *130*, 16330–16337.
24. Bethell, D.; Fessey, R. E.; Namwindwa, E.; Roberts, D. W. The Hydrolysis of C_{12} Primary Alkyl Sulfates in Concentrated Aqueous Solutions. Part 1. General Features, Kinetic Form and Mode of Catalysis in Sodium Dodecyl Sulfate Hydrolysis. *J. Chem. Soc., Perkin Trans. 2* **2001**, 1489.
25. Sun, Z.; Nicolosi, V.; Rickard, D.; Bergin, S. D.; Aherne, D.; Coleman, J. N. Quantitative Evaluation of Surfactant-Stabilized Single-Walled Carbon Nanotubes: Dispersion Quality and Its Correlation with Zeta Potential. *J. Phys. Chem. C* **2008**, *112*, 10692–10699.
26. Lebedkin, S.; Hennrich, F.; Kiowski, O.; Kappes, M. M. Photophysics of Carbon Nanotubes in Organic Polymer−Toluene Dispersions: Emission and Excitation Satellites and Relaxation Pathways. *Phys. Rev. B* **2008**, *77*, 165429-1-8.